

Human influences on the present denudation rates of the Paulista Peripheral Depression, Brazil

Alexandre Martins Fernandes ^a, Fabiano Tomazini da Conceição ^{a,*}, Eder Paulo Spatti Júnior ^a, Antonio Aparecido Couto Júnior ^a, Christophe Hissler ^b, Jefferson Mortatti ^c

^a UNESP – Universidade Estadual Paulista - Instituto de Geociências e Ciências Exatas, Rio Claro, São Paulo, Brazil

^b Catchment and Eco-hydrology group – Luxembourg Institute of Science and Technology, Luxembourg

^c Centro de Energia Nuclear na Agricultura - Universidade de São Paulo, Piracicaba, São Paulo, Brazil

ARTICLE INFO

Article history:

Received 7 May 2019

Received in revised form 7 November 2019

Accepted 7 November 2019

Available online 9 November 2019

Keywords:

Landscape evolution

Water-rock interactions

Human-landscape system

Brazil

ABSTRACT

Chemical weathering and soil erosion in large or small watersheds are used to understand the effect of evolution processes on the Earth's surface and climate. Currently, human-driven land use changes have substantial effects on landscape changes over a range of temporal and spatial scales. In this context, the Sorocaba River basin, São Paulo State, Brazil, is an ideal study area to assess human influence on the present denudation rates of the Paulista Peripheral Depression (PPD). Twelve fluvial water sample collections were carried out at the Sorocaba River mouth, covering one complete hydrological cycle (Jun/2009 to Jun/2010). In the same period, 46 rainfall events were sampled. All samples were analyzed for dissolved cations, anions and silica, and total dissolved solids (TDS). Total suspended solids (TSS) were measured only in fluvial samples. The export of TDS and TSS occurs mostly during the wet season, accounting for ca. 60% and 87% of the total dissolved solids and total suspended sediment transported in the hydrological cycle studied (2009/2010), respectively. The total annual specific flux of TSS was 74.27 t/km²/year (including soil erosion by agricultural activities), with a small portion being derived from the anthropogenic contributions (ca. 2%). The total annual specific flux of TDS (74.43 t/km²/year) was similar to the TSS, but after the correction of the atmospheric inputs and anthropogenic contributions (ca. 18 and 29%, respectively), this value decreased to 39.35 t/km²/year. The chemical weathering rate was 7.1 m/Myer and this process tended towards monosalitization ($R_E = 2.6$), with an atmospheric/soil CO₂ consumption rate of 3.3×10^{-5} mol/km²/year. The difference between the chemical weathering and soil removal rates (7.1 and 49.6 m/Myer, respectively) indicated that the soil thickness reduction occurred in the Sorocaba River basin. The climatic control on chemical weathering and soil removal rates was clearly evidenced, with the highest values of denudation occurring in the wet and hot climatic conditions. However, the chemical weathering processes (R_E index) was not sensitive to climatic controls. In order to assess human influence on chemical weathering and soil removal rates in the PPD, the results were compared with other works undertaken in this vast geomorphological province. Even considering the uncertainties associated with a number of data points, the chemical weathering and soil removal rates in the PPD observed in this study were approximately 4 and 7.5-fold higher than these natural denudation rates, respectively, evidencing the effect of recent land use changes on the present denudation rates in the PPD. Thus, this study reinforces the complexity of the human-landscape systems in São Paulo State and increases the values of long-term landscape evolution rates.

© 2019 Elsevier B.V. All rights reserved.

1. Introduction

The dissolved and suspended loads carried by rivers to the oceans are generally related to several processes and interactions involving climatic, hydrological, physical, chemical and biological conditions. Chemical weathering is a typically a destructive process, where the primary minerals of the bedrock are chemically weathered in secondary

minerals due to chemical reactions from the joint action of water and the atmospheric/soil CO₂. This process releases the soluble ions that supply the dissolved load to the rivers and the residual products of the chemical weathering provide the materials that constitute the soil profile (Millot et al., 2002). On the other hand, soil erosion promotes a reduction in the soil thickness and the material removed is subject to the transportation and sedimentation processes. The sediment load (suspended load and bed load) carried by the rivers is related to the soil erosion. In this work, the sediments load will be considered only as the suspended load. In synthetic terms, chemical weathering supplies

* Corresponding author.

E-mail address: fabiano.tomazini@unesp.br (F.T. da Conceição).

the dissolved load to rivers, whereas soil erosion supplies the solid loads, and these processes play an important role in the evolution of the Earth's surface (Négrel et al., 2007). Thus, the present denudation rates can be measured using the dissolved and suspended load carried by rivers.

The watershed is characterized as an important unit for conducting hydrochemical studies related to chemical weathering and soil removal rates. The changes that occur in the drainage area are reflected in the quality of surface water and can be evidenced by the monitoring of river systems (Mortatti and Probst, 2003) from the assessment of loads of cations, anions and dissolved silica and suspended particulate matter. The first studies to investigate the nature and composition of the suspended and dissolved load transported by rivers were carried out in the 1960s and 1970s (e.g., Barth, 1961; Gibbs, 1967, 1970; Johnson et al., 1968; Tardy, 1968, 1969, 1971; Martin and Meybeck, 1979). Since then, many studies have been developed, including those that used mass balance models and adjusted atmospheric and anthropogenic contributions where necessary, to identify the fractions from the soil denudation and/or rock weathering processes and determine their respective rates (e.g., Meybeck, 1987; Stallard and Edmond, 1987; Lasaga et al., 1994; White and Blum, 1995; Gaillardet et al., 1997, 1999; Boeglin and Probst, 1998; Dessert et al., 2001; Millot et al., 2002; Dessert et al., 2003; Mortatti and Probst, 2003; Oliva et al., 2003; Walling and Fang, 2003; West et al., 2005; Louvat et al., 2008; Moon et al., 2014).

However, the natural landscape evolution has been modified by different human activities (Murray et al., 2009). These human-landscape systems generate several impacts on the temporal and spatial scales (Harden et al., 2014). Land use/land cover changes (LULCC) are responsible for the increase of soil erosion, a process naturally influenced by the climate, soil, vegetation, and relief (Summerfield, 1991). Montgomery (2007) proposed that the soil removal rates in plowed agricultural fields are 1–2 orders of magnitude greater than rates of soil production, erosion under native vegetation and long-term geological erosion. Studies on land use changes have been developed in America, Asia, Africa and Europe (Van Rompaey et al., 2002; Latocha and Migon, 2006; Latocha, 2009; Mhangara et al., 2012; Mugagga et al., 2012; Bruschi et al., 2013; García-Ruiz et al., 2013; Kim et al., 2014; Sanyal et al., 2014; Sun et al., 2014; Gessesse et al., 2015; Karamesouti et al., 2015; Serpa et al., 2015; Hernández et al., 2016; Kosmas et al., 2016; Latocha et al., 2016; Tarolli and Sofia, 2016; Zhang and Shangguan, 2016; Zope et al., 2016). In Brazil, only a few studies have documented the impacts of land use changes in rural or urban areas (Rodrigues, 2005; Costa and Bacellar, 2007; Simon and Cunha, 2008; Beskow et al., 2009; Latrubesse et al., 2009; Minella et al., 2009; Perez Filho and Quaresma, 2011; Moraes et al., 2012; Oliveira et al., 2015; Rosolen et al., 2015; Borrelli et al., 2017; Lupinacci et al., 2017; Couto Júnior et al., 2019).

Precambrian Cratons, Orogenic Belts and Phanerozoic Sedimentary Basins are the main geodynamic structures in Brazil territory, with different Geomorphological Provinces (Fig. 1a). Three geomorphological provinces have been recognized locally in the São Paulo State: the Atlantic Plateau (AP), the Paulista Peripheral Depression (PPD) and the Occidental Plateau (OC) (Fig. 1b). According to Almeida (1964), the PPD was formed during the Neogene and Pleistocene periods, between the Paraná CFB (continental flood basalt) province of the Paraná Basin and the igneous/metamorphic rocks of Mantiqueira Orogenic Belt (Fig. 1b) and mainly consists of clastic sedimentary rocks from the Paraná Basin, and represents a sculpted. The Sorocaba River basin (Fig. 1c) is located in the southeastern part of the São Paulo State. Since its occupation in the seventeenth century, the Sorocaba River basin has gone through successive cycles of development and has seen the diversification of human activities, and is currently under strong anthropic pressure, with a population of ca. 1 million inhabitants, 1850 enterprises and large agricultural areas (IPT, 2006; IBGE, 2010). The LULCC in the Sorocaba River basin may affect the present denudation rates in

this watershed, the mouth of which is located in the PPD. Thus, this work aims to assess human influences on the present chemical weathering and soil removal rates in the PPD, obtained through dissolved and suspended loads, respectively, and carried by Sorocaba River.

2. Study area

The Sorocaba River basin covers an area of 5269 km² and is located between latitudes 23 and 24°S and longitudes 47 and 48°W (Fig. 1c). The average annual temperature ranged from 18 to 22 °C (IPT, 2006). According to the Köppen (1948) classification, the climate is a Cwa type, characterized by the predominance of higher values of rainfall and discharge in the summer period (October to March) in relation to dry periods (April to September). The pluviometric and fluviometric historical data (DAEE, 2010) of the study area for the 50-year period (1959 to 2008) are illustrated in Fig. 2a, showing that January was the month with the highest values of rainfall (215 mm) and discharge (107.1 m³/s), while August presented the lowest values of rainfall (32 mm) and discharge (35.5 m³/s). The significant positive relationship between the monthly average rainfall and discharge for the same period was obtained ($r = 0.786, P < .01$) from those 50 years (Fig. 2b).

The Sorocaba River basin is located in two distinct geomorphological provinces (Fig. 1c). The AP province is associated with metamorphic rocks and granitoid complexes belonging to the São Roque Group and Embu Complex (Godoy et al., 1996). The PPD province outcrops the clastic sedimentary rocks from the Paraná Basin related to Itararé, Guatá and Passa Dois groups (Conceição and Bonotto, 2004; IPT, 2006). The relief in the AP is comprised of hills shapes with convex tops and deep valleys with altitudes that range between 800 and 1000 m and high-density drainage channels that have slope above 20%; in the PPD, this is represented by hills with tabular and large convex tops, prevailing altitudes between 600 and 700 m and slopes ranging between 5 and 10% (Ross and Moroz, 1997; Perrota et al., 2005).

Red Argisol (49%), Red Latosol (38%) and Red-Yellow Latosol (9%) are the predominant soils in the Sorocaba River basin (Oliveira et al., 1999), according to the Brazilian soil classification (EMBRAPA, 2013) and corresponding to Ultisols and Oxisols in the USDA nomenclature (USDA, 1999), respectively. The original vegetation, characterized by forests, brushwood, fields and lowland Savanna vegetation, was replaced by anthropogenic pastures and fields (77%), agricultural crops (14%), urban areas (4%) and reforestation areas (3%) due to the agricultural occupation and urbanization processes, leaving only 2% of the original vegetation cover remaining.

3. Methods

According to Moon et al. (2014), the assessment of chemical weathering and soil removal rates is necessary to consider the sampling frequency and variability in the river discharge, concentration and contribution of different sources. In the same study, the author suggests at least 10 and preferably 40 temporal chemical data points with synchronous discharge from each river, with uncertainties within –28 to 22%, –22 to 16% and –14 to 15% with 10, 24 and 40 samples (50% confidence). Twelve fluvial water samples were collected at the Sorocaba River (Fig. 1c), covering one complete hydrological cycle (Jun/2009 to Jun/2010), and representing the extremes of the rainfall and discharge regimes (Fig. 2). River waters were collected and separated into two 500 mL aliquots, one crude for analyzing dissolved cations and anions and the other preserved with 0.1 mL of concentrated H₂SO₄ only for analyzing dissolved SiO₂.

The instantaneous discharge (Q) during the sampling was calculated from the product of the wet river channel cross-section area (m²), obtained by bathymetry, and the average velocity of the water flow in

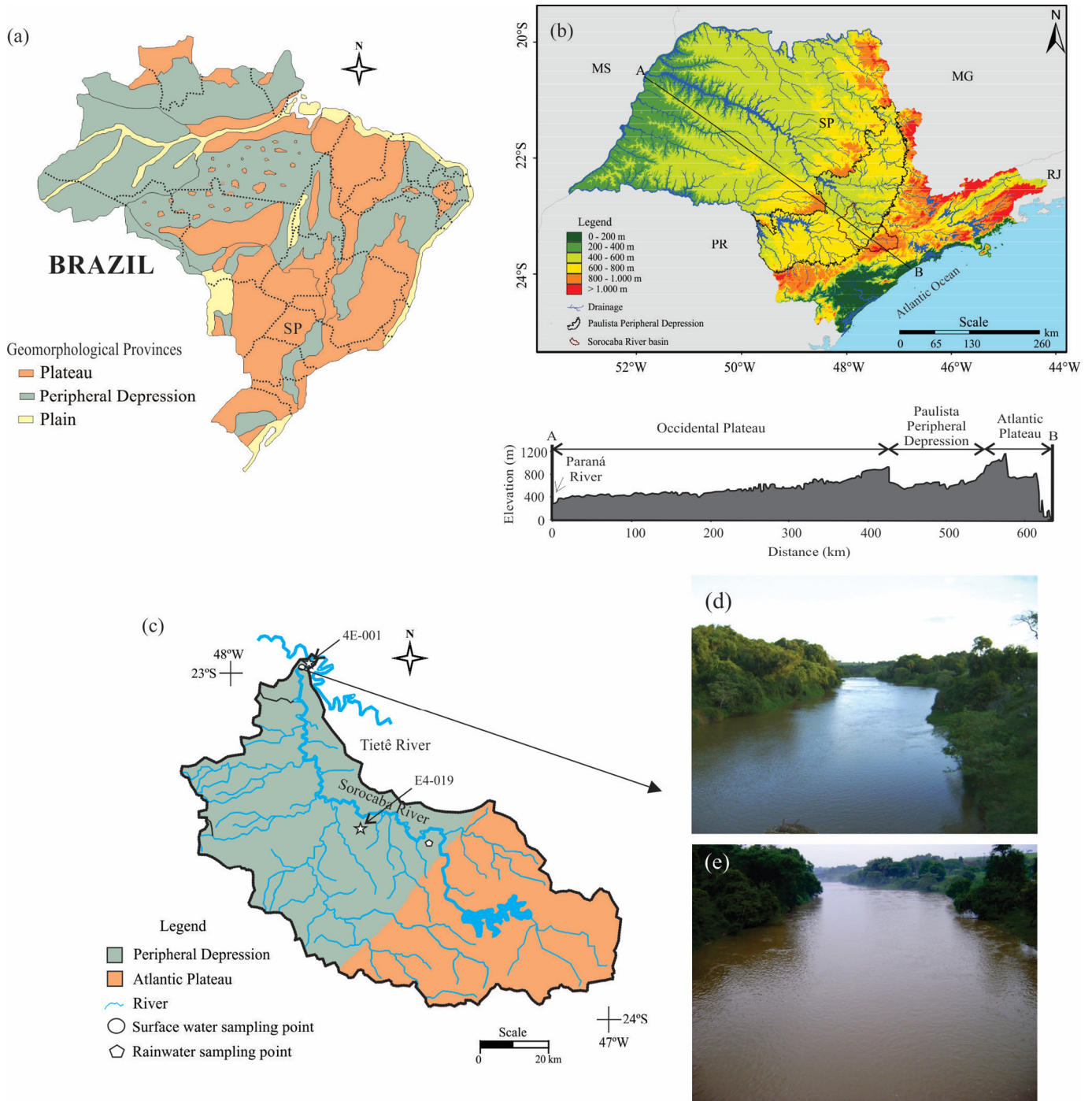


Fig. 1. Geomorphological Provinces in Brazil (a) (Ross, 1985). A digital elevation model (USGS, 2011) for São Paulo State, with a ca. 600 km long topographic transverse from the Paraná River to the Atlantic Ocean shows distinct geomorphological provinces, according to Almeida (1964), where SP, RJ, MG, MS and PR are the states of São Paulo, Rio de Janeiro, Minas Gerais, Mato Grosso de Sul e Paraná, respectively (b). The location of the fluvial sampling point at the mouth of the Sorocaba River basin (23°03'53"S and 47°49'13"W), the pluvial sampling point in the central portion of the watershed and the pluviometric E4-019 (23°20'S and 47°41'W) and pluviometric 4E-001 (23°01'S and 47°48'W) stations (c). View of the sampling location during the dry season in July 2009 (d) and the rainy season in January 2010 (e).

this section (m/s), using a Digital Micromolinet Global Water FP 101. The pH values were measured using a DM2 Digimed portable pH; and a DM3 Digimed sensor was used in the characterization of electrical conductivity (EC) and temperature (T), with both pieces of equipment calibrated with Digimed standard solutions.

The samples (crude and preserved) were filtered, using a cellulose membrane filter (0.45 µm), previously dried and weighed. The crude filtered samples were analyzed by ion chromatography (Dionex ICS-90), calibrated with Dionex standard solutions and equipped with the

analytical columns IonPac® CS12A 4 × 250 mm and IonPac® AS14A 4 × 250 mm, for the concentration quantification of dissolved cations (Na⁺, K⁺, Ca²⁺ and Mg²⁺) and anions (Cl⁻, SO₄²⁻, PO₄³⁻ and NO₃⁻), with a quantification limit of 10 µg/L (Ribani et al., 2004) and detection limit of 1 µg/L (Dionex Corporation, 2004). The alkalinity was measured using the Gran method (Edmond, 1970), using standardized HCl (0.1 N) in the titration. The preserved samples were used in the quantification of dissolved Si⁴⁺ concentration by optical emission spectrometry with inductively coupled argon plasma (Optima 3000 DV), with a

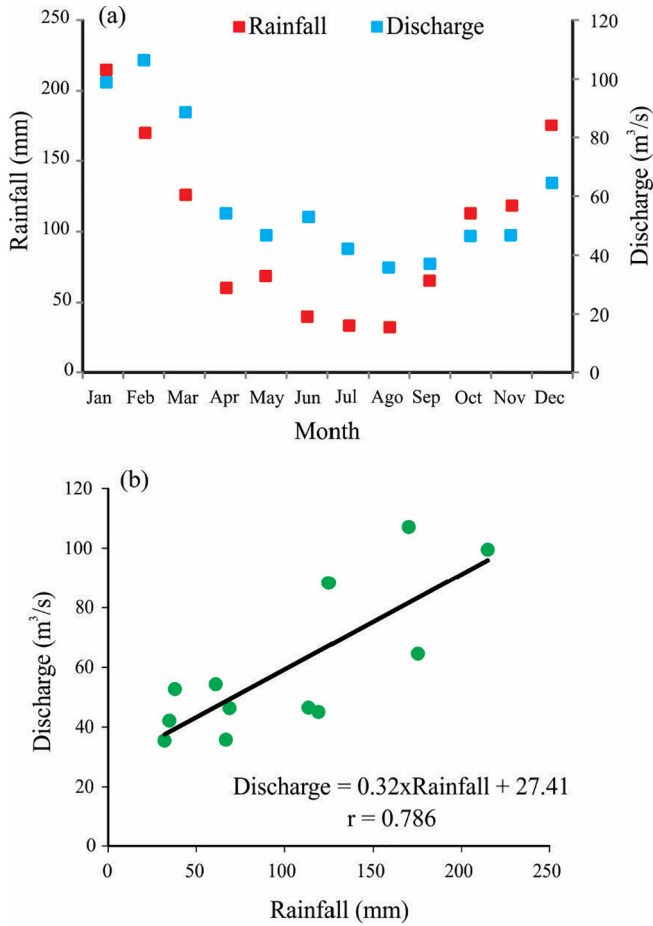


Fig. 2. Monthly average rainfall and discharge for a 50-year period (1959–2008) in the Sorocaba River basin (a), obtained from the DAEE (2010).

detection limit of 20 $\mu\text{g/L}$. The sum of dissolved ions and silica was considered as the total dissolved solids (TDS). The total suspended solids (TSS) were quantified gravimetrically (APHA, 1999). The discharge weighted averages (C_{WAV} – in mg/L) to the dissolved chemical species, TDS and TSS were calculated according to Eq. (1).

$$C_{WAV} = \frac{\sum_{i=1}^n C_i \cdot Q_i}{\sum_{i=1}^n Q_i} \quad (1)$$

where: C_i = ion concentration in the sample i (mg/L). Q_i = discharge in the sampling i (m^3/s).

Rainfall events were sampled during the same period ($n = 46$), using a pluviometer (“bulk” type - dry and wet deposition) (Fig. 1c). Each rain event was represented by precipitation that occurred during a 24-hour period and the total volume was measured using a graduated calibrated cylinder. After measuring the pH value, the rainwater sample was stored in two 100 mL polyethylene bottles, one with the crude sample and the other with the preserved sample with concentrated H_2SO_4 , and both were kept refrigerated at 4 °C. The rainwater was analyzed in terms of dissolved ions (crude sample) and SiO_2 (preserved sample), using the same analytical procedure described for river water samples. The concentrations were synthesized in terms of a rainfall-weighted average for the study period (R_{WAV} – in mg/L), and dry and wet periods, and were calculated according to Eq. (1), where the instantaneous discharge parameter was replaced by the rainfall volume in the event. All events were considered using a normalized inorganic charge balance (NICB) proposed by Mosello et al. (1996).

4. Theoretical background

4.1. Contribution of different sources to fluvial fluxes

The contribution of different sources to fluvial fluxes of dissolved cations, anions and silica, as well as the TSS and TDS, were calculated using a mass balance model expressed in Eq. (2), modified from White and Blum (1995). The model used did not consider the fluxes resulting from the biomass change and derived from the ionic exchange sites in clay minerals because they have negligible contributions, close to “zero”, according to White and Blum (1995).

$$F_W = F_{river} - F_{rainfall} - F_{anthropogenic} \quad (2)$$

where: F_W = flux associated with chemical weathering or soil erosion ($\text{t}/\text{km}^2/\text{year}$). F_{river} = river flux ($\text{t}/\text{km}^2/\text{year}$). $F_{rainfall}$ and $F_{anthropogenic}$ = atmospheric and anthropogenic inputs ($\text{t}/\text{km}^2/\text{year}$).

The F_{river} and $F_{rainfall}$ were obtained according to Eq. (3) (Probst, 1992) and Eq. (4), respectively.

$$F_{river} = \frac{C_{WAV} \cdot \bar{Q}}{A} \quad (3)$$

$$F_{rainfall} = \frac{R_{WAV} \cdot P}{1000} \quad (4)$$

where: \bar{Q} = average discharge of the study period (m^3/s). A = surface area of the watershed (km^2). P = total precipitation in the study period (mm).

The $F_{anthropogenic}$ for dissolved load related to urban sewage was calculated considering the anthropogenic influences in the Upper Sorocaba River basin (Sardinha et al., 2008), presented by the authors as percentages of the concentration ion in the total fluvial flux (F_{river}), i.e., 35% calcium, 23% magnesium, 65% sodium, 10% potassium, 14% alkalinity, 53% sulfate, 36% nitrate, 91% chlorine and 54% phosphate. The $[\text{SiO}_2]$ in urban sewage can be disregarded, as suggested by Mortatti et al. (2012). The $F_{anthropogenic}$ for suspended load, the anthropogenic contribution, was represented by product of the per capita TSS load contained in untreated urban sewage (0.022 kg/hab/day), obtained from an average production of untreated urban sewage (100 L/hab/day) and the respective TSS average concentration (220 mg/L) (Tchobanoglous and Burton, 1991), the urban sewage treatment percentage in the Sorocaba River basin, estimated at 25% (IPT, 2006) and the total population of 1,212,376 inhabitants (IBGE, 2010).

4.2. Chemical weathering processes and CO_2 consumption

The predominant process in the chemical weathering of the rocks can be determined using the R_E index (Tardy, 1968, 1971), modified by Boeglin and Probst (1998) (Eq. (5)). This index is equivalent to the molecular ratio (SiO_2)/(Al_2O_3) of secondary minerals neo-formation within the soil profile and is expressed by the molar ratio of chemical dissolved species in the surface waters, i.e. silica and cations resulting from the rock weathering. The predominant process is characterized according to a classification proposed by Pedro (1966), where $R_E \approx 0$ characterize the total hydrolysis process known as alitization, with aluminum and iron fixed as insoluble hydroxides; $R_E \approx 2$ is related to the partial hydrolysis of minerals and monosalitization is the predominant process, with kaolinite formation; and $R_E \approx 4$ is the occurrence of partial hydrolysis with the bisalutization process and the formation of mineral 2:1, such as montmorillonite.

$$R_E = \frac{3K + 3Na + 2Ca + 1.25Mg - \text{SiO}_2}{0.5K + 0.5Na + Ca + 0.75Mg} \quad (5)$$

The atmospheric/soil CO₂ consumption rate (F_{CO_2} in mol/km²/year) associated with chemical weathering was estimated using Eq. (6) (Gaillardet et al., 1999; Mortatti and Probst, 2003).

$$F_{CO_2} = F_{Na\ sil} + F_{K\ sil} + 2 F_{Ca\ sil} + 2 F_{Mg\ sil} \quad (6)$$

where: $F_{(ion)sil} = F_w$ of Na⁺, K⁺, Ca²⁺ and Mg²⁺ (mol/km²/year).

4.3. Chemical weathering and soil removal rates

The fluvial flux related to the rock weathering process was estimated as the sum of the fluvial transport of cations and SiO₂ (IQ in t/km²/year), after the correction of atmospheric inputs and anthropogenic contributions, according to Eq. (7) (Probst, 1992). The chemical weathering rate (W_q in m/Myear) can be calculated using Eq. (8).

$$IQ = F_w(Na^+) + F_w(K^+) + F_w(Ca^{2+}) + F_w(Mg^{2+}) + F_w(SiO_2) \quad (7)$$

$$W_q = \frac{IQ}{\rho} \quad (8)$$

where: $F_w(ion)$ = corrected annual fluvial flux of the Na⁺, K⁺, Ca²⁺, Mg²⁺ and SiO₂. ρ = the mean density of rocks in the watershed.

The soil erosion rate (W_m in m/Myear) can be expressed as the ratio of the TSS annual flux and the superficial soil density (ρ'), as suggested by Boeglin and Probst (1998) and expressed in Eq. (9).

$$W_m = \frac{F_{TSS}}{\rho'} \quad (9)$$

5. Results

5.1. Chemistry of surface waters

The results of Q, pH, EC, T and concentrations of dissolved ions, SiO₂, TDS and TSS, with their respective averages for the study period, are in Table 1. The Q values showed seasonal variation in consonance with the historical data of the monthly average (Fig. 2), with an average discharge for the study period of 146.62 m³/s. The Sorocaba River waters presented a pH ranging from 6.9 to 7.3 during the study period (average of 7.0). The EC showed significant seasonal variation (average of 110.8 μ S/cm), with values below 80 μ S/cm in the months of highest rainfall and discharge, and values above 140 μ S/cm during the dry season (Jun/2009 and Jun/2010). The river water temperature followed

the annual cycle (average of 23.2 °C), with lower values in winter (15.6 °C in Jun/2009) and higher values in summer (33.0 °C in Jan/2010).

The [TSS] was directly related to the discharge (Fig. 3a). For most rivers worldwide, the b exponent in the $[TSS] = a.Q^b$ model is positive and has values between 1 and 2 (Probst, 1986). The model established for the Sorocaba River presented b as equal to 0.792, suggesting that [TSS] was influenced by both discharge and rainfall. The higher [TSS] occurred in Mar/2010 (178.00 mg/L) and Nov/2009 (145.00 mg/L), after rainfall events of 27.5 and 13.5 mm, respectively, corroborating this influence. The relationship between the [TDS] and the Q was inverse and significant (Fig. 3b), representing the dilution process with increasing Q values. The percentage distribution of the dissolved ions in relation to the TDS, on a molar basis (Peray, 1998), indicated the predominance of HCO₃⁻ among the anions (31%), followed by Cl⁻, NO₃⁻, SO₄²⁻ and PO₄³⁻, while for the cations the greatest participation was Na⁺, with 22%, followed by Ca²⁺, Mg²⁺ e K⁺, respectively, and the SiO₂ represented 12% of the TDS. The charge balance, represented by the relationship “sum of cation concentrations vs sum of anion concentrations”, in μ eq/L, indicated a deficit of anionic charges (Fig. 3c), which can be related to dissolved organic anions not counted in this study, such as dissolved organic carbon (Probst et al., 1992).

5.2. Atmospheric loading

The results of rainwater chemical analysis are presented in Table 2 (all results are illustrated in Fig. 4). The pH values ranged from 5.0 to 6.7 (average of 5.7). The SiO₂ concentrations showed values below the detection limit, since the atmospheric inputs of dissolved silica are minimal (White and Blum, 1995). Among the chemically dissolved ions, the Ca²⁺ and HCO₃⁻ accounted for 81% of the cations sum and 62% of anions sum, respectively. The dissolved cations showed the following distribution trend: Ca²⁺ > Na⁺ > Mg²⁺ > K⁺, whereas for the anions the trend was HCO₃⁻ > SO₄²⁻ > Cl⁻ > NO₃⁻ > PO₄³⁻. Both trends were maintained in the dry and wet periods, and differences in average concentrations between these periods may be related to the sampled event number in each period, the dilution effect on rainfall volume function and the atmospheric “washout” effect induced for successive rainfall events (Moreira-Nordemann et al., 1997).

Ionic ratios obtained for the rainwater in the Sorocaba River basin (Ca²⁺/Na⁺ = 8.70, Mg²⁺/Na⁺ = 0.57, K⁺/Na⁺ = 0.42, SO₄²⁻/Na⁺ = 1.50 and HCO₃⁻/Na⁺ = 6.18) indicated low marine influence when compared to the rainwater ionic ratios observed near the sea (0.04, 0.23, 0.02, 0.12 and <0.01, respectively – Wilson, 1975), given that individual systematic surveys indicate no significant spatial variations

Table 1
Physical and chemical results for the Sorocaba River surface waters.

Unit	Sampling date												C _{WAV}	
	06/09	07/09	08/09	09/09	11/09	12/09	01/10	02/10	03/10	04/10	05/10	06/10		
Q	m ³ /s	37.47	43.71	123.23	99.84	170.01	363.35	366.47	184.04	151.30	107.64	70.21	42.15	146.62
pH		6.9	6.9	6.9	7.1	6.9	6.9	7.1	7.1	7.3	7.1	7.1	7.3	7.0
EC	μ S/cm	143.2	123.9	109.0	121.8	108.1	76.0	79.7	99.6	87.1	103.6	128.6	149.1	110.8
T	°C	15.6	16.9	16.9	20.3	26.4	25.7	33.0	29.0	26.8	24.7	22.2	21.1	23.2
SiO ₂	mg/L	35.90	31.00	14.12	17.50	11.89	10.43	10.44	12.45	11.49	12.21	22.00	29.00	13.61
Ca ²⁺	mg/L	16.70	16.36	11.75	13.54	10.0	8.40	8.50	10.50	11.11	13.35	13.26	13.69	10.63
Mg ²⁺	mg/L	1.52	1.47	1.08	1.05	1.00	0.84	0.82	1.20	1.25	1.30	1.40	1.90	1.06
Na ⁺	mg/L	27.18	23.67	10.61	11.16	10.20	5.70	6.03	7.70	7.70	9.14	14.92	18.83	9.03
K ⁺	mg/L	1.82	1.70	1.45	1.47	1.40	1.00	1.10	1.70	1.70	1.80	1.90	2.10	1.40
HCO ₃ ⁻	mg/L	47.52	42.00	34.66	42.30	34.40	26.73	30.95	39.20	31.94	40.28	41.08	46.34	34.24
Cl ⁻	mg/L	17.20	16.30	8.48	8.54	8.19	4.20	4.33	5.87	5.95	7.02	11.27	12.23	6.71
SO ₄ ²⁻	mg/L	9.95	9.10	5.05	5.36	5.40	4.80	3.23	3.36	4.40	5.04	6.22	10.34	4.82
NO ₃ ⁻	mg/L	10.55	8.88	2.74	3.26	2.78	0.93	0.96	3.96	4.50	5.98	8.25	10.14	3.22
PO ₄ ³⁻	mg/L	0.60	0.47	0.15	0.12	<0.01	0.09	<0.01	<0.01	0.22	0.11	0.33	0.37	0.11
TDS	mg/L	169.11	150.95	90.09	104.29	86.06	63.12	66.35	85.94	80.25	96.24	120.61	144.94	84.82
TSS	mg/L	14.33	46.50	54.33	45.33	145.00	87.17	101.50	37.83	178.00	51.00	22.67	14.50	84.83

Q = discharge; EC = electrical conductivity; T = temperature; TDS = total dissolved solids; TSS = total suspended sediments; C_{WAV} = weighted average element/compound concentration for the study period.

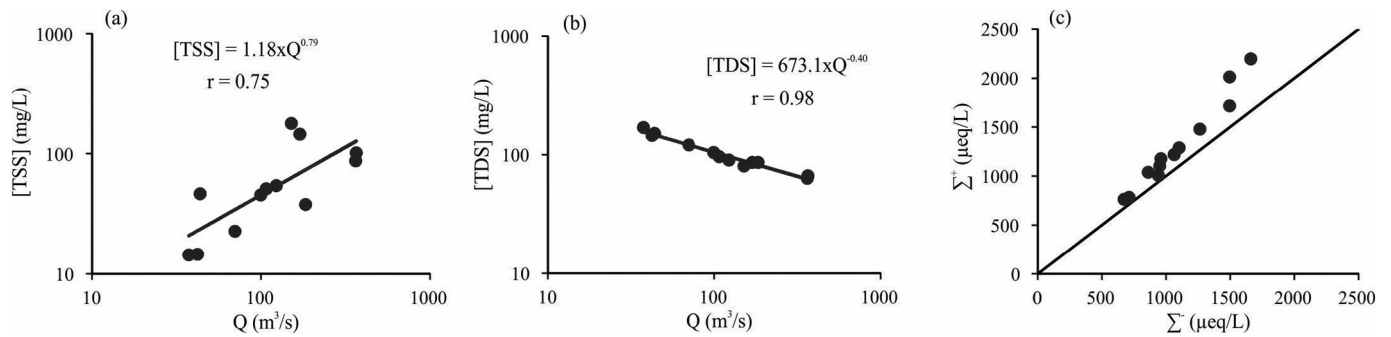


Fig. 3. Relationships between discharge and [TSS] (a) and between discharge and [TDS] (b), and charge balance in the Sorocaba River in the study period, with Σ^+ and Σ^- corresponding to the total dissolved cations and anions, respectively (c).

among fractions in marine rainfall (Keene et al., 1986). Despite the similarity of the Cl^-/Na^+ rainwater ratio (1.17) with cyclic salts and marine aerosols (1.16 – Wilson, 1975), other ionic ratios reflected the predominance of terrestrial influences on the chemical composition in the Sorocaba River basin rainwater, as already verified in the Sorocaba City by Conceição et al. (2013).

6. Discussion

6.1. Seasonality and contribution of different sources to fluvial fluxes

The fluvial fluxes integrate the contributions of the chemical weathering and soil removal that occur in the watershed, and also the atmospheric inputs and, in some regions, the anthropogenic inputs associated with pollution from industrial, agricultural and/or urban activities, which can reach the river in punctual or diffuse contribution forms (Stallard and Edmond, 1981; Probst et al., 1994; Mortatti et al., 1997; Conceição and Bonotto, 2004; Hissler and Probst, 2006; Conceição et al., 2015a; Hissler et al., 2015, 2016; Fernandes et al., 2016). The total fluvial fluxes of TDS and TSS were similar (ca. 74 t/km²/year), with the value of specific flux related to soil erosion considered as the medium specific sediment flux (50 to 200 kg/km²/day) (Meybeck et al., 2003). Fig. 5 illustrates the instantaneous daily flux, which can be calculated using the values of [TDS], [TSS] and Q , suggesting that the majority of the TDS and TSS are carried during the summer period due to the South Atlantic Convergence Zone, which provides high intensity rainfall events in southeastern Brazil.

The fluvial fluxes associated with chemical weathering or soil removal (F_w) were calculated using Eq. (2). In order to obtain the F_{river} (Eq. (3)), we used C_{WAV} of dissolved chemical species, TDS and TSS

Table 2
Results of rainwater chemical analysis in the Sorocaba River basin.

	R_{WAV}	Min	Max	Dry	Wet	R_{WAV}
	(mg/L)					(μeq/L)
pH	5.7	5.0	6.7	5.6	6.1	–
SiO ₂	<0.02	<0.02	<0.02	<0.02	<0.02	–
Ca ²⁺	1.42	0.26	3.37	2.08	1.10	71.21
Mg ²⁺	0.09	0.01	0.30	0.09	0.04	4.65
Na ⁺	0.19	0.04	0.94	0.27	0.15	8.19
K ⁺	0.13	0.01	0.57	0.16	0.12	3.44
HCO ₃ ⁻	3.08	0.10	4.71	3.53	2.71	50.60
Cl ⁻	0.34	0.01	1.85	0.47	0.27	9.55
SO ₄ ²⁻	0.59	0.03	2.33	0.93	0.42	12.32
NO ₃ ⁻	0.56	0.01	2.60	0.84	0.42	9.07
PO ₄ ³⁻	0.02	0.01	0.16	0.03	0.02	0.73
Σ cations	–	–	–	–	–	87.49
Σ anions	–	–	–	–	–	82.27

R_{WAV} = weighted average volume; Min = minimum value; Max = maximum value; Dry = weighted average volume in dry period; Wet = weighted average volume in wet period.

values and the average discharge presented in Table 1 and the area of the Sorocaba River basin (5269 km²), while for $F_{rainfall}$ (Eq. (4)), we used the total precipitation in the study period (2101 mm) and the R_{WAV} of dissolved chemical species (Table 2). The $F_{anthropogenic}$ of the dissolved and particulate loads were calculated as previously described. In Fig. 6, it is possible to observe a significant influence of anthropogenic sources in the composition of surface waters from the Sorocaba River basin.

As mentioned by Conceição and Bonotto (2004) and Fernandes et al. (2016), only silicate minerals are presented in the igneous/metamorphic and sedimentary rocks in the watershed studied. Thus, it was not necessary to consider the influence of carbonate and evaporite rocks in the mass-balance model used in this study (Eq. (2)). The values of F_w , F_{river} , $F_{rainfall}$ and $F_{anthropogenic}$ are presented in Table 3 (t/km²/year) and in Fig. 7 (%). Only Cl^- and PO_4^{3-} yielded negative values, whereas a positive mass-balance was found for the other element/compounds, i.e. 2.38 t/km²/year of Na⁺, 3.07 t/km²/year of Ca²⁺, 0.60 t/km²/year of Mg²⁺, 0.83 t/km²/year of K⁺, 11.94 t/km²/year of SiO₂, 19.35 t/km²/year of HCO₃⁻, 0.75 t/km²/year of SO₄²⁻, 0.63 t/km²/year of NO₃⁻ and 39.35 t/km²/year of TDS. The chemical weathering of silicate, atmospheric and anthropogenic inputs account for 53, 18 and 29% of the annual dissolved load in the Sorocaba River, respectively. The annual suspended solids load was 72.77 t/km²/year.

6.2. Water-rock interactions and chemical weathering and soil removal rates

The predominant chemical weathering process of these rocks in the Sorocaba River basin was determined using the R_E (Eq. (5)). The value of 2.6 obtained characterized the predominance tendency of partial hydrolysis of the primary silicate minerals (Fig. 8). In general, the main minerals found in the igneous, metamorphic and sedimentary rocks described in the Sorocaba River basin were studied by Conceição and Bonotto (2004) and Fernandes et al. (2016):

- The Embu Complex (migmatitic gneisses) is composed of biotite ($K(Mg,Fe)_3(Si_3Al)O_{10}(OH)_2$), muscovite ($KAl_2(Si_3Al)O_{10}(OH)_2$) and sillimanite (Al_2SiO_5), quartz (SiO_2), microcline ($KAlSi_3O_8$) and oligoclase ($(Na,Ca)(Si,Al)_4O_8$);
- The São Roque Group rocks (metarhytmities) presented quartz, muscovite and biotite;
- Granitoid rocks are comprised of quartz, microcline and oligoclase, biotite and hornblende ($Ca_2Na(Mg,Fe)_4(Al,Fe,Ti)AlSi_8AlO_{22}(OH)_2$);
- Sedimentary rocks possess quartz, albite ($NaAlSi_3O_8$), microcline, kaolinite ($Al_2Si_2O_5(OH)$) and illite ($K_{0.9}Al_2Si_4O_{10}(OH)_2$).

Thus, considering the monossialization process occurring in the Sorocaba River basin, the annual fluxes of Na⁺ have their origin in the

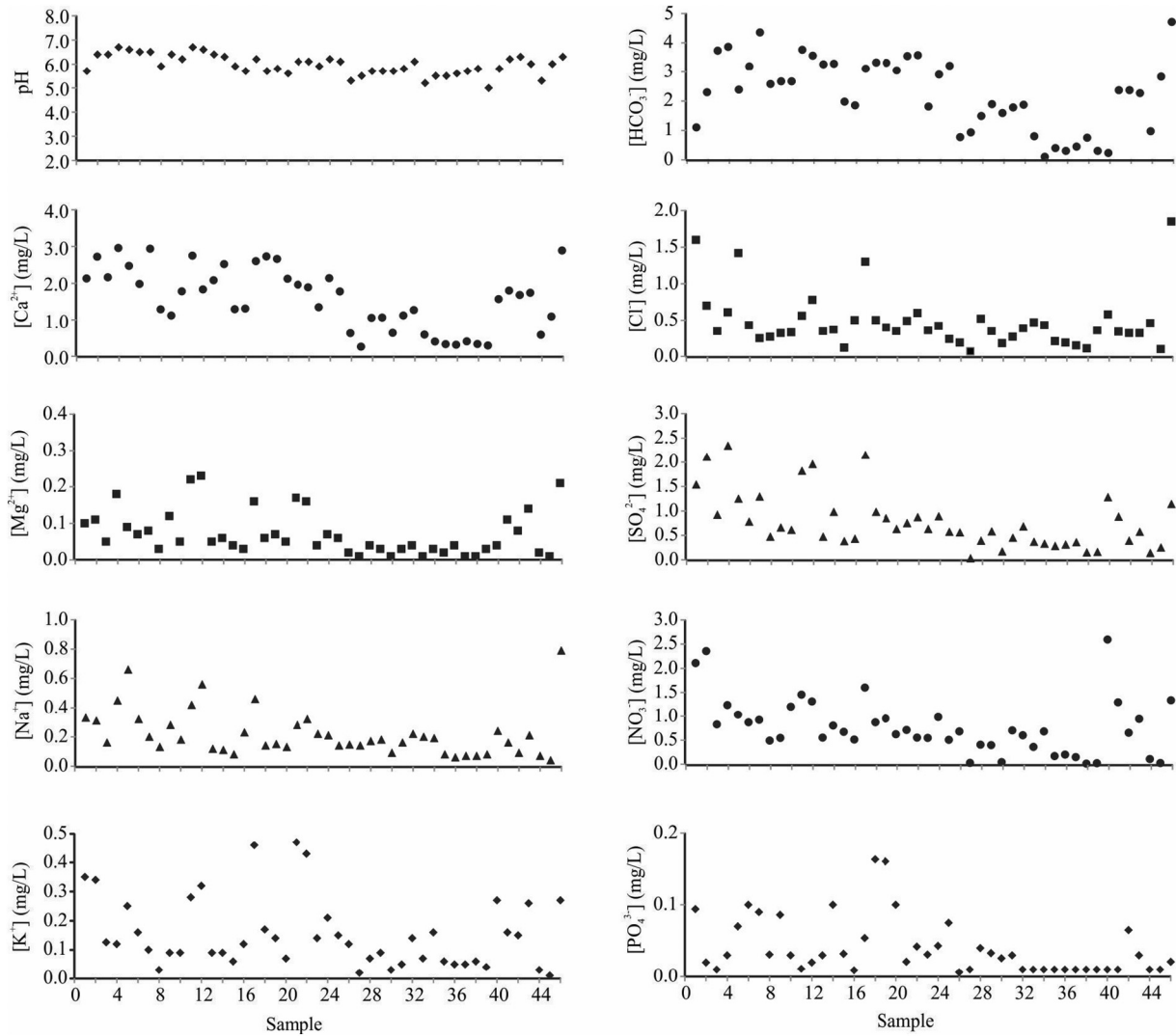


Fig. 4. All results of pH and dissolved cations and anions measured in rainwaters in the Sorocaba River basin.

hydrolysis of albite, hornblende and plagioclase; K^+ ions are derived from the hydrolysis of muscovite, microcline, biotite and illite; Ca^{2+} can be attributed to the hydrolysis of hornblende and plagioclase; and Mg^{2+} can be released by the hydrolysis of hornblende and biotite. Quartz and a kaolinite are not weathered and remain in the soil profile (with goethite - $FeOOH$ and rutile - TiO_2).

The atmospheric/soil CO_2 consumption rate, calculated via silicate weathering (Eq. (6)), was 3.3×10^5 mol/ km^2 /year. According to Meybeck (1987), the world continental average of atmospheric/soil

CO_2 consumption rate is 1.61×10^5 mol/ km^2 /year, which is lower than the value obtained in this study. In addition, this value is higher than other South American watersheds, such as the basins of the Amazonas (0.3×10^5 mol/ km^2 /year - Mortatti and Probst, 2003), Orinoco (0.7×10^5 mol/ km^2 /year - Gaillardet et al., 1999) and Jamari and Jiparana (0.8×10^5 and 1.4×10^5 mol/ km^2 /year, respectively - Mortatti et al., 1992). It is, however, lower than in carbonate areas (0.8×10^6 mol/ km^2 /year - Meybeck, 1987) and basaltic watersheds worldwide, i.e. on São Miguel island - Azores (0.6×10^6 mol/ km^2 /year - Louvat and Allègre, 1998), in Iceland (0.7×10^6 mol/ km^2 /year - Louvat et al., 2008), in the Deccan Traps (1.3×10^6 mol/ km^2 /year - Dessert et al., 2001), on Réunion Island (2.3×10^6 mol/ km^2 /year - Louvat and Allègre, 1997) and in the Paraná continental flood basalts (0.4×10^6 mol/ km^2 /year, Conceição et al., 2015b).

The IQ in the Sorocaba River basin (Eq. (7)) corresponded to 18.8 t/ km^2 /year, representing 48% of the TDS flux at the river mouth. Using Eq. (8) and considering that the mean density of rocks (ρ) in this watershed is 2.65 g/ cm^3 (Brasil, 1983), it was possible to calculate a chemical weathering rate (Wq) of 7.1 m/Myear. In addition, the soil removal rate (W_m) of 49.6 m/Myear was estimated according Eq. (9), using the TSS annual flux (Table 3) and the soil density (1.47 g/ cm^3 - Fernandes et al., 2012). Considering the chemical weathering and soil removal rates, a reduction of soil thickness of ca. 42.5 m/Myear can be obtained in the Sorocaba River basin. This value is in accordance with the global balance usually accepted for watersheds, where the soil

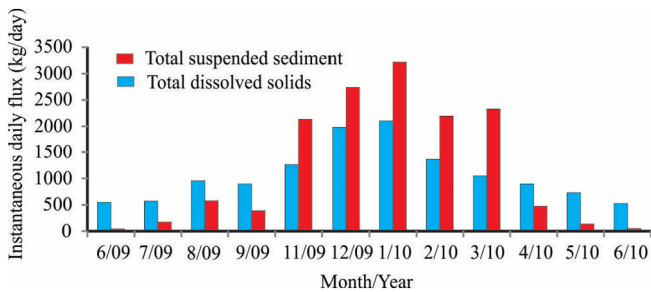


Fig. 5. Instantaneous daily flux of total dissolved solids (TDS) and total suspended solids (TSS) in the Sorocaba River basin, indicating that this parameter is directly related to discharge, in accordance with most world rivers (Bernier and Bernier, 1987).

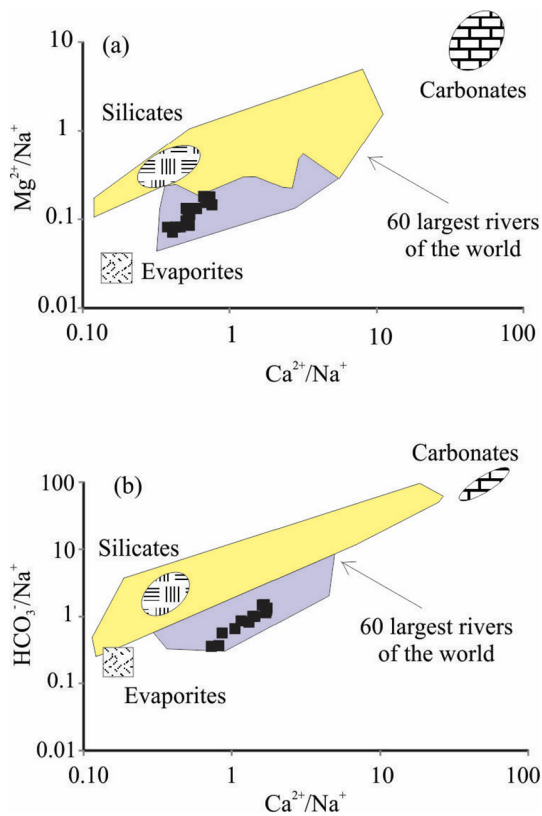


Fig. 6. The Na-normalized molar ratio diagrams in the dissolved phase of the Sorocaba River, with the end member reservoirs representing the small watershed with a single lithology (carbonates, silicates and evaporates) and the 60 large rivers around the world (Gaillardet et al., 1999). The polluted rivers are gray to distinguish them from the others.

erosion rates are approximately six times higher than the chemical weathering rate (Lasaga et al., 1994).

6.3. Climatic control on chemical weathering and soil removal rates

Besides the lithology, the chemical weathering and soil removal rates have a direct relationship with climatic conditions, mainly rainfall and temperature, in a watershed (Meybeck, 1987; White and Blum, 1995; Gaillardet et al., 1999; Oliva et al., 2003). However, relief, land cover and water time residence in the weathering profiles are also important factors in these assessments (Oliva et al., 2003; West et al., 2005). The tropical climate in the Sorocaba River basin is characterized by the predominance of rainfall in summer and dryness in winter, with the rainfall possessing a significant positive relationship with the discharge (Fig. 2). This fact indicates that months with lower rainfall and temperature values have lower discharge values, and vice versa.

Thus, in order to assess the climatic control on the chemical weathering (W_q) and soil removal (W_m) rates in the Sorocaba River basin, a modelling consisting of the use of 12 scenarios was proposed. The rates in each scenario were calculated assuming the values of instantaneous discharge, [TSS] and [cations + SiO_2] obtained in each sampling as the annual average, allowing us to understand the climatic control since from driest to wettest years. The anthropogenic influences

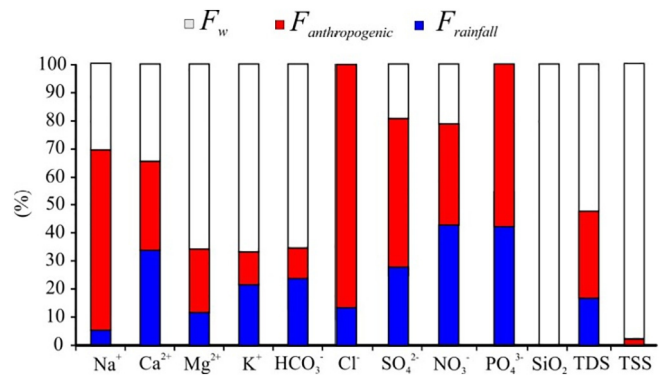


Fig. 7. Contribution of different sources (%) to dissolved cations, SiO_2 , HCO_3^- and TDS in the Sorocaba River. F_w = natural flux due to chemical weathering, $F_{anthropogenic}$ = anthropogenic influences, $F_{rainfall}$ = the atmospheric inputs.

were corrected as previously discussed. The atmospheric inputs were obtained through the monthly [cations + SiO_2] and annual rainfall from the monthly average values registered over a 50-year period (1959–2008) (DAEE, 2010), i.e.: June = 453 mm; July = 416 mm; August = 384 mm; September = 801 mm; November = 1431 mm; December = 2105 mm; January = 2579 mm; February = 2041 mm; March = 1498 mm; April = 732 mm and May = 826 mm. In addition, the chemical weathering processes (R_E index) were also modelled using the 12 scenarios proposed.

Fig. 9 illustrates the modelled results in each scenario (W_q , W_m and R_E) and the values measured in this study. The highest values of W_q and W_m were modelled in wet scenarios, reaching up to 10 times the difference between the rates. However, in dry scenarios, the values of W_q and W_m decreased and the chemical weathering rates were higher than the soil removal rates. The chemical weathering and soil removal rates possess similar values (6.3 m/Year) in scenario related to discharge of ca. $47 \text{ m}^3/\text{s}$. Thus, the scenarios proposed show clearly the climatic control on chemical weathering and soil removal rates, with the highest values of denudation occurring in the wet and hot climatic conditions (highest values of rainfall) and in dry and hot climatic conditions the denudation rates would be more moderate.

In addition, it is interesting to note that the values of W_q and W_m measured in this study are perfectly adjusted in the linear regression model presented in Eqs. (10) and (11). In addition, significant values of the coefficient of determination ($r = 0.99$ for the W_q and $r = 0.89$ for the W_m) were obtained, even considering the deviation of the data points within the mid-range in relation to the trend of the best-fit line for W_m . Thus, the equations proposed during the modelling (Fig. 9a) can be used in the Sorocaba River basin to obtain indirectly the values of W_q and W_m , in years with rainfall ranging from 384 to 2579 mm.

$$W_q = 0.042.Q + 3.996 \quad (r = 0.99) \quad (10)$$

$$W_m = 0.433.Q - 13.991 \quad (r = 0.89) \quad (11)$$

Unlike the climatic control on the chemical weathering and soil removal rates, the chemical weathering processes (R_E index) indicated the partial hydrolysis of primary silicate minerals during all scenarios modelled, independently of the climatic conditions. Tardy (1971)

Table 3

The annual flux (t/km²/year) of dissolved cations, anions and silica, total suspended solids (TSS) and total dissolved solids (TDS) in the Sorocaba River basin.

Species	SiO_2	Ca^{2+}	Mg^{2+}	Na^+	K^+	HCO_3^-	Cl^-	SO_4^{2-}	NO_3^-	PO_4^{3-}	TDS	TSS
F_{river}	11.94	9.33	0.93	7.93	1.23	30.04	5.89	4.23	2.83	0.09	74.43	74.29
$F_{rainfall}$	–	2.99	0.12	0.4	0.28	6.48	0.71	1.24	1.18	0.05	13.45	–
$F_{anthropogenic}$	–	3.27	0.21	5.15	0.12	4.21	5.36	2.24	1.02	0.05	21.63	1.52
F_w	11.94	3.07	0.60	2.38	0.83	19.35	–0.18	0.75	0.63	–0.01	39.35	72.77

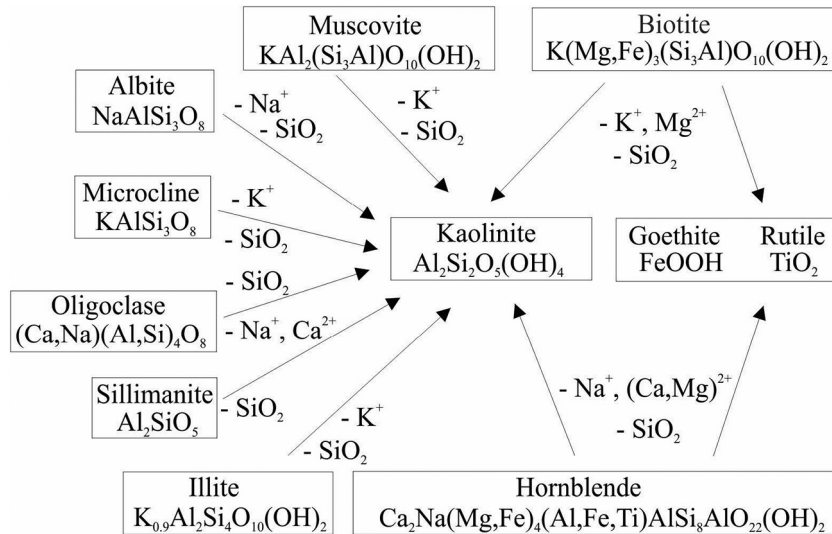


Fig. 8. Theoretical weathering reactions involving the mineral constituents of the igneous, metamorphic and sedimentary rocks (Fernandes et al., 2016; Conceição and Bonotto, 2004) in the Sorocaba River basin.

explains that the chemical composition of surface waters is sensitive to climatic controls (temperature and rainfall) and, consequently, the annual seasonality can interfere with and change the denudation rates, but does not modify the chemical weathering processes. Thus, the results of this study confirm that the annual seasonality does not represent a significant climatic change that would affect the chemical

weathering processes in the Sorocaba River basin, as suggested by Tardy (1971).

6.4. Human influences on the present denudation rates in the Paulista Peripheral Depression

In order to investigate the present denudation rates in the Paulista Peripheral Depression, a mass-balance among the fluvial transport in the Sorocaba River mouth and each Geomorphological Province (Atlantic Plateau - AP and Paulista Peripheral Depression - PPD) can be used (Eqs. (12) and (13)). Table 4 reports the parameters necessary to obtain the IQ (7.0 t/km²/year) and F_{TSS} (97.4 t/km²/year) values, which were used in the estimation of the present denudation rates in the PPD. Thus, utilizing these values and Eqs. (6) and (7), the chemical weathering and soil removal rates in the PPD were 2.7 and 66.3 m/Myer, respectively. Using uncertainties of -28 to 22% due to the number of data points (12) used in this study, as suggested by Moon et al. (2014), the chemical weathering and soil removal rates can vary from 2.0 to 3.3 m/Myer and 47.8 to 80.9 m/Myer, respectively.

$$Q_{SRM} \cdot [\text{cations} + \text{SiO}_2]_{SRM} = Q_{AP} \cdot [\text{cations} + \text{SiO}_2]_{AP} + Q_{PPD} \cdot [\text{cations} + \text{SiO}_2]_{PPD} \tag{12}$$

$$Q_{SRM} \cdot [TSS]_{SRM} = Q_{AP} \cdot [TSS]_{AP} + Q_{PPD} \cdot [TSS]_{PPD} \tag{13}$$

where: Q_{SRM} , Q_{AP} and Q_{PPD} = discharge in the Sorocaba River mouth, Atlantic Plateau and Paulista Peripheral Depression (m³/s), respectively. $[\text{cations} + \text{SiO}_2]_{SRM}$, $[\text{cations} + \text{SiO}_2]_{AP}$ and $[\text{cations} + \text{SiO}_2]_{PPD}$ = fluvial transport of cations and SiO₂ in the Sorocaba River mouth, Atlantic Plateau and Paulista Peripheral Depression (mg/L), respectively. $[TSS]_{SRM}$, $[TSS]_{AP}$ and $[TSS]_{PPD}$ = TSS annual flux in the Sorocaba River

Table 4
Area, discharge (Q) and natural values of [TSS] and [cations and SiO₂] in the Sorocaba River basin.

	Area (km ²)	Q (m ³ /s)	[TSS] (mg/L)	[cations + SiO ₂]
Sorocaba River mouth	5269	146.62	83.13	21.42
Paulista Peripheral Depression	3161	85.05	114.81	8.30
Atlantic Plateau ^a	2108	61.57	43.41	39.57

^a Data reported by Fernandes (2012).

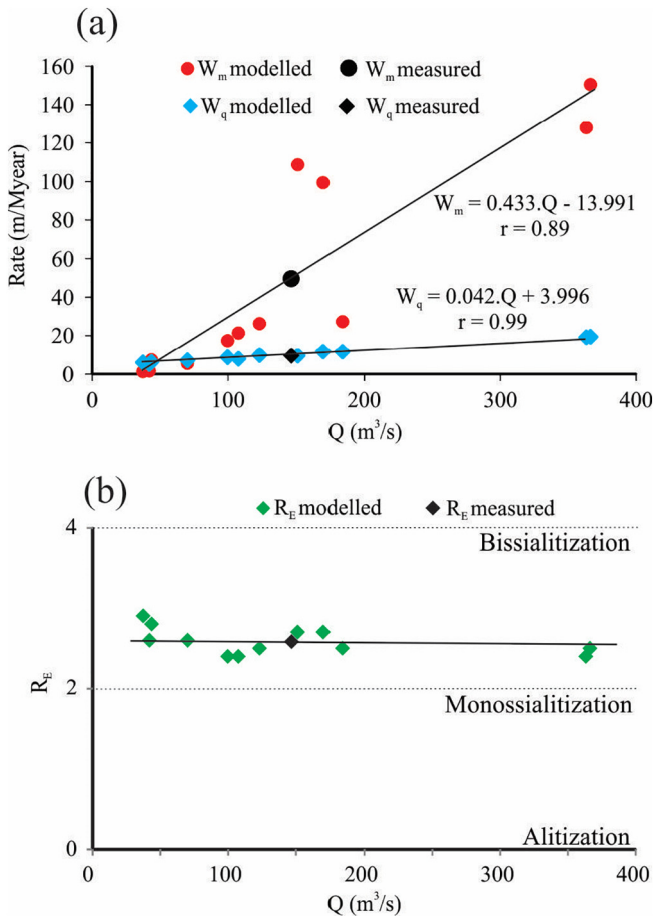


Fig. 9. Chemical weathering and soil removal rates (a) and RE index (b) modelled in the Sorocaba River basin.

mouth, Atlantic Plateau and Paulista Peripheral Depression (mg/L), respectively.

The chemical weathering rates obtained for the clastic sedimentary rocks in the PPD (2.7 m/Myer) are higher than the calculated for the igneous/metamorphic rocks belong to Ribeira Belt in the AP (15 m/Myer – Fernandes et al., 2016) and for the Paraná CFB province in the OP (6 m/Myer – Conceição et al., 2015b), other important geological units in the São Paulo State (Fig. 1b). In general, evaporites and carbonates weather faster than silicate rocks, with igneous (granites and basalts) and metamorphic (schists and gneisses) rocks having higher chemical weathering rates than clastic sedimentary rocks (sandstones, siltstones and mudstones) (Oliva et al., 2003). This study confirms that igneous/metamorphic and basaltic rocks weather faster than clastic sedimentary rocks in the São Paulo State, which possesses minerals with higher resistance to chemical weathering (mainly quartz and kaolinite), according to the Goldich dissolution series (Goldich, 1938).

As discussed in this work, the fluvial fluxes associated with chemical weathering in the Sorocaba River basin are directly affected by human activities, which theoretically should be corrected using the model proposed by White and Blum (1995 – Equation 2). Studies of chemical weathering rates in small watersheds with one single type of rock allow an understanding the influence of the lithology on the chemical weathering rates (Millot et al., 2002). Unfortunately, there are no studies in small watersheds in the Sorocaba River basin reporting on the chemical weathering rate related to the clastic sedimentary rocks in the PPD. Thus, in order to verify the possible human influence on the chemical weathering rates in the PPD, it was necessary to compare the chemical weathering rate obtained in this study with other rates measured in small watersheds located in the PPD.

Spatti Júnior et al. (2019) studied the chemical weathering processes of the clastic sedimentary rocks in the PPD, using two small watersheds composed mainly for sandstone and mudstone (Monjolo Grande and Jacutinga watersheds, respectively), and indicated an average chemical weathering rate of ca. 0.6 m/Myer. Couto Junior et al. (2016) determined, through fluvial geochemistry in the Cachoeirinha Stream basin, chemical weathering rates of 0.7 m/Myer for sandstone and mudstone in the PPD. Thus, even considering the uncertainties of the chemical weathering rate of clastic sedimentary rocks in the PPD observed in this study, this rate was ca. 4-fold higher than proposed in the studies conducted in small watersheds composed mainly for sandstone and mudstone located in the PPD (Couto Junior et al., 2016; Spatti Júnior et al., 2019).

In relation to the soil removal rates, in the São Paulo State there are no watersheds with natural vegetation cover that could be used as a control site unaffected by human activities to assess the natural removal soil rates in the PPD. In addition, long-term soil removal rates related to the PPD in São Paulo State are also not documented and cannot be compared to present rates, since this stable cratonic region has remained at practically the same tropical position since the South Atlantic reactivation in the Lower Cretaceous (Hasui, 2010). However, Riffel et al. (2015) proposed the long-term landscape evolution of the Second Paraná Plateau, a unit correspondent to the PPD in the Paraná State, using a combined $^{40}\text{Ar}/^{39}\text{Ar}$ (Mn oxyhydroxides) and (U–Th)–He (goethites) geochronology. In this study, the authors suggested that the weathering processes started at 35 Myer and were particularly intense during the Miocene (17–8 Myer), with a Post-Eocene soil removal rate of ca. 9 m/Myer. The present soil removal rate in the PPD (66.3 m/Myer, ranging from 47.8 to 80.9 m/Myer considering the uncertainties associated with the number of data points) was almost 7.5-fold higher than the Post-Eocene soil removal rates, clearly indicating human influence on the soil removal rates.

It is evident that the LULCC are responsible for serious environmental problems on the local, regional and global scale, which can undermine the capacity of ecosystems to sustain food production,

maintain freshwater and forest resources, regulate climate and air quality (Foley et al., 2005). Particularly in the São Paulo State, the LULCC are associated with the production of biofuels, which are responsible for 42% of the renewable energy supply in Brazil (OECD/FAO, 2015). In addition, the agricultural land and pastures areas in the PPD have been changed for sugar cane crops due to a growing demand for ethanol since the Brazilian federal government implemented the PRO-ALCÓOL Project started in 1975 (Adami et al., 2012). A recent study conducted by Couto Júnior et al. (2019) indicated that this change for sugar cane crops can increase soil loss by ca. 270% in relation to the current land use. Thus, this study has shown that human landscape systems affect denudation rates in the PPD and, with the continuous expansion of sugar cane crops in the PPD, denudation rates may increase further in the future due to the Brazilian energy policy.

7. Conclusion

This study allowed a better understanding of the chemical weathering of rocks and the soil erosion processes that occur in a tropical region of South America, through the evaluation of the fluvial transport dynamics in the Sorocaba River basin. The concentration of dissolved cations, anions and silica increased during the period with lower discharge. The most abundant cations and anions in surface waters were Ca^{2+} and HCO_3^- . The TSS concentration was directly related to the discharge and influenced by rainfall, with higher concentrations recorded after rainfall events, while for the TDS concentration this relationship was inverted, showing dilution behavior. The export of TDS and TSS occurs mostly during the wet season, accounting for ca. 60% and 87% of the total dissolved solids and total suspended sediment transported in the hydrological cycle studied (2009/2010), respectively. For the total annual specific flux of TSS (74.27 t/km²/year), a small portion was derived from the anthropogenic contributions (ca. 2%), with the flux related to the soil erosion process estimated at 72.77 t/km²/year. The TDS showed a total annual specific flux of 74.43 t/km²/year, similar to the TSS, and after the atmospheric and anthropogenic corrections (ca. 18 and 29%, respectively), the TDS flux related to the chemical weathering was 39.35 t/km²/year. The chemical weathering rock process showed a tendency towards monosalitization ($R_E = 2.6$), with an atmospheric/soil CO₂ consumption rate of 3.3×10^5 mol/km²/year. The chemical weathering and soil removal rates in the Sorocaba River basin were 7.1 and 49.6 m/Myer, respectively, indicating the soil thickness reduction. The modelling of climatic control on chemical weathering and soil removal rates suggested that the highest values of denudation occurring in the wet and hot climatic conditions (highest values of rainfall), but do not affect the chemical weathering processes. Even considering the uncertainties associated with chemical weathering and soil removal rates, the effect of recent land use changes on the present denudation rates in the PPD is evident. In relation to the chemical weathering rates, even with the corrections made, the model used here for assessing these rates still presents problems related to anthropogenic influences, reinforcing the need for the use of small watershed in the future studies involving the chemical weathering rates of rocks, specifically. As for soil removal rates, the human landscape systems are affecting the natural processes of soil removal, and, consequently, the landscape evolution in the PPD. Thus, the results provide new knowledge related to human-landscape systems in vast Geomorphological Provinces, knowledge which should be used elsewhere to better understand human influence on the present denudation rates. In addition, future studies comparing present soil removal rates, obtained from an extensive and systematic geochemical mass-balance, with Cenozoic long-term soil removal rates, using $^{40}\text{Ar}/^{39}\text{Ar}$ and (U–Th)–He geochronology, must be carried out in the PPD, allowing us to assess whether the soil removal rates were constant or episodic during the Cenozoic.

Declaration of competing interest

The authors declare that they have no known competing financial interests or personal relationships that could have appeared to influence the work reported in this paper.

Acknowledgments

The authors are grateful to the Fundação de Amparo à Pesquisa do Estado de São Paulo (Process No. 08/57104-4 and 08/09369-9), and to the Conselho Nacional de Desenvolvimento Científico e Tecnológico, (Process No. 134169/2009-3) for their financial support, and to the Stable Isotope Laboratory of the Center for Nuclear Energy in Agriculture, São Paulo, Brazil for the research infrastructure. In particular, Dr. Achim A. Beylich and two anonymous referees are thanked for their detailed and insightful review comments, which have helped to improve the manuscript.

References

- OECD/FAO, 2015. OECD-FAO Agricultural Outlook 2015. OECD Publishing, Paris https://doi.org/10.1787/agr_outlook-2015-en.
- Adami, M., Rudorff, B.F.T., Freitas, R.M., Aguiar, D.A., Sugawara, L.M., Mello, M.P., 2012. Remote sensing time series to evaluate direct land use change of recent expanded sugarcane crop in Brazil. *Sustainability* 4, 574–585. <https://doi.org/10.3390/su4040574>.
- Almeida, F.F.M., 1964. Fundamentos geológicos do relevo paulista. *Boletim do Instituto Geográfico e Geológico* 41, 169–263.
- APHA (Ed.), 1999. Standard Methods for the Examination of Water and Wastewater, 20 ed Washington D.C, APHA.
- Barth, T.F.W., 1961. Abundance of the elements, areal averages and geochemical cycles. *Geochim. Cosmochim. Acta* 23, 1–8. [https://doi.org/10.1016/0016-7037\(61\)90086-2](https://doi.org/10.1016/0016-7037(61)90086-2).
- Berner, E.K., Berner, R.A., 1987. *The Global Water Cycle: Geochemistry and Environment*. Prentice-Hall, New Jersey.
- Beskow, S., Mello, C.R., Norton, L.D., Curi, N., Viola, M.R., Avanzi, J.C., 2009. Soil erosion prediction in the Grande River Basin, Brazil using distributed modeling. *Catena* 79, 49–59. <https://doi.org/10.1016/j.catena.2009.05.010>.
- Boeglin, J.J., Probst, J.L., 1998. Physical and chemical weathering rates and CO₂ consumption in a tropical lateritic environment: the upper Niger basin. *Chem. Geol.* 148, 137–156. [https://doi.org/10.1016/S0009-2541\(98\)00025-4](https://doi.org/10.1016/S0009-2541(98)00025-4).
- Borrelli, P., Robinson, D.A., Fleischer, L.R., Lugato, E., Ballabio, C., Alewell, C., Bagarello, V., 2017. An assessment of the global impact of 21st century land use change on soil erosion. *Nat. Commun.* 8 (1), 1–13. <https://doi.org/10.1038/s41467-017-02142-7>.
- Bruschi, V.M., Bonachea, J., Remondo, J., Gómez-Arozamena, J., Rivas, V., Méndez, G., Naredo, J.M., Cendrero, A., 2013. Analysis of geomorphic systems' response to natural and human drivers in northern Spain: implications for global geomorphic change. *Geomorphology* 196, 267–279. <https://doi.org/10.1016/j.geomorph.2012.03.017>.
- Conceição, F.T., Bonotto, D.M., 2004. Weathering rates and anthropogenic influences in a sedimentary basin, São Paulo State, Brazil. *Appl. Geochem.* 19, 575–591. <https://doi.org/10.1016/j.apgeochem.2003.07.002>.
- Conceição, F.T., Antunes, M.L.P., Angelucci, V.A., Moruzzi, R.B., Navarro, G.R.B., 2013. Rain-water chemical composition and annual atmospheric deposition in Sorocaba, (São Paulo State), Brazil. *Rev. Bras. Geophys.* 31 (1), 5–15. <https://doi.org/10.1590/rbfg.v31n1.242>.
- Conceição, F.T., Sardinha, D.S., Godoy, L.H., Fernandes, A.M., Pedrazzi, F.J.M., 2015a. Influência sazonal no transporte específico de metais totais e dissolvidos nas águas fluviais da Bacia do Alto Sorocaba (SP). *Geochim. Bras.* 29 (1), 23–34. <https://doi.org/10.5327/Z1012-9800201500010003>.
- Conceição, F.T., Santos, C.M., Sardinha, D.S., Navarro, G.R.B., Godoy, L.H., 2015b. Chemical weathering rate, denudation rate, and atmospheric and soil CO₂ consumption of Paraná flood basalts in São Paulo State, Brazil. *Geomorphology* 233, 41–51. <https://doi.org/10.1016/j.geomorph.2014.10.040>.
- Dionex Corporation, 2004. ICS-90 ion chromatography system operator's manual. California: Dionex Corporation. (Document n.031851, revision 4).
- Costa, F.M., Bacellar, L.D.A.P., 2007. Analysis of the influence of gully erosion in the flow pattern of catchment streams, Southeastern Brazil. *Catena* 69, 230–238. <https://doi.org/10.1016/j.catena.2006.05.007>.
- Couto Junior, A.A., Conceição, F.T., Fernandes, A.M., Lupinacci, C.M., Spatti Junior, E.P., 2016. Geoquímica fluvial aplicada à avaliação das taxas de intemperismo químico e remoção de solo da Formação Rio Claro. *Rev. Bras. Geomorfologia* 17(3), 451–464. doi:10.20502/rbg.v17i3.1006.
- Couto Júnior, A.A., Conceição, F.T., Fernandes, A.M., Spatti Júnior, E.P., Lupinacci, C.M., Moruzzi, R.B., 2019. Land use changes associated with the expansion of sugar cane crops and their influences on soil removal in a tropical watershed in São Paulo State (Brazil). *Catena* 172, 313–323. <https://doi.org/10.1016/j.catena.2018.09.001>.
- DAEE, 2010. Banco de dados hidrológicos. <http://www.hidrologia.dae.sp.gov.br/> (accessed 16 June 2015).
- Dessert, C., Dupré, B., François, L.M., Schott, J., Gaillardet, J., Chakrapani, G., Bajpai, S., 2001. Erosion of Deccan Traps determined by river geochemistry: impact on the global climate and the ⁸⁷Sr/⁸⁶Sr ratio of seawater. *Earth Planet. Sci. Lett.* 188, 459–474. [https://doi.org/10.1016/S0012-821X\(01\)00317-X](https://doi.org/10.1016/S0012-821X(01)00317-X).
- Dessert, C., Dupré, B., Gaillardet, J., François, L.M., Allègre, C.J., 2003. Basalt weathering laws and the impact of basalt weathering on the global carbon cycle. *Chem. Geol.* 202, 257–273. <https://doi.org/10.1016/j.chemgeo.2002.10.001>.
- Edmond, J.M., 1970. High precision determination of titration alkalinity and total carbon dioxide content of seawater by potentiometric titration. *Deep-Sea Research Part I: Oceanogr. Res. Pap.* 17 (4), 737–750. [https://doi.org/10.1016/0011-7471\(70\)90038-0](https://doi.org/10.1016/0011-7471(70)90038-0).
- EMBRAPA, Empresa Brasileira de Pesquisa Agropecuária, 2013. *Sistema brasileiro de classificação de solos*. 3.ed. EMBRAPA, Brasília.
- Fernandes, A.M., 2012. Características hidrogeoquímicas da bacia de drenagem do rio Sorocaba, SP: processos erosivos mecânicos e químicos. *Doctoral Thesis*. Universidade de São Paulo, São Paulo, Brazil.
- Fernandes, A.M., Nolasco, M.B., Hissler, C., Mortatti, J., 2012. Mechanical erosion in a tropical river basin in Southeastern Brazil: chemical characteristics and annual fluvial transport mechanisms. *J. Geol. Res.* v.2012, Article ID 127109, 8 pages. doi:10.1155/2012/127109.
- Fernandes, A.M., Conceição, F.T., Spatti Junior, E.P., Sardinha, D.S., Mortatti, J., 2016. Chemical weathering rates and atmospheric/soil CO₂ consumption of igneous and metamorphic rocks under tropical climate in southeastern Brazil. *Chem. Geol.* 443, 54–66. <https://doi.org/10.1016/j.chemgeo.2016.09.008>.
- Foley, J.A., DeFries, R., Asner, G.P., Barford, C., Bonan, G., Carpenter, S.R., Helkowski, J.H., 2005. Global consequences of land use. *Science* 309, 570–574. <https://doi.org/10.1126/science.1111772>.
- Gaillardet, J., Dupré, B., Allègre, C.J., Négrel, P., 1997. Chemical and physical denudation in the Amazon river basin. *Chem. Geol.* 142, 141–173. [https://doi.org/10.1016/S0009-2541\(97\)00074-0](https://doi.org/10.1016/S0009-2541(97)00074-0).
- Gaillardet, J., Dupré, B., Louvat, P., Allègre, C.J., 1999. Global silicate weathering and CO₂ consumption rates deduced from the chemistry of large rivers. *Chem. Geol.* 159, 3–30. [https://doi.org/10.1016/S0009-2541\(99\)00031-5](https://doi.org/10.1016/S0009-2541(99)00031-5).
- García-Ruiz, J.M., Nadal-Romero, E., Lana-Renault, N., Beguería, S., 2013. Erosion in Mediterranean landscapes: changes and future challenges. *Geomorphology* 198, 20–36. <https://doi.org/10.1016/j.geomorph.2013.05.023>.
- Gessesse, B., Bewket, W., Bräuning, A., 2015. Model-based characterization and monitoring of runoff and soil erosion in response to land use/land cover changes in the Modjo watershed, Ethiopia. *Land Degrad. Develop.* 26, 711–724. <https://doi.org/10.1002/ldr.2276>.
- Gibbs, R.J., 1967. The geochemistry of the Amazon River System. Part 1. The factors that control the salinity and composition and concentration of suspended solids. *Geol. Soc. Am. Bull.* 78, 1203–1232. [https://doi.org/10.1130/0016-7606\(1967\)78\[1203:TGOTAR\]2.0.CO;2](https://doi.org/10.1130/0016-7606(1967)78[1203:TGOTAR]2.0.CO;2).
- Gibbs, R.J., 1970. Mechanisms controlling world river water chemistry. *Science* 170, 1088–1090. <https://doi.org/10.1126/science.170.3962.1088>.
- Godoy, A.M., Hackspacher, P.C., Oliveira, M.A.F., 1996. *Geologia da folha Sorocaba*. *Geociências* 15, 89–110.
- Goldich, S.S., 1938. A study in rock weathering. *J. Geol.* 46, 17–58. <https://doi.org/10.1086/624619>.
- Harden, C.P., Chin, A., English, M.R., Fu, R., Galvin, K.A., Gerlak, A.K., McDowell, P.F., McNamara, D.E., Peterson, J.M., Poff, N.L., Rosa, E.A., Solecki, W.D., Wohl, E.E., 2014. Understanding human-landscape interactions in the “Anthropocene”. *Environ. Manag.* 53, 4–13. <https://doi.org/10.1007/s00267-013-0082-0>.
- Hasui, Y., 2010. A grande colisão pré-cambriana do sudeste brasileiro e a estruturação regional. *Geociências* 29 (2), 141–169.
- Hernández, A., Arellano, E., Morales-Moraga, D., Miranda, D.D., 2016. Understanding the effect of three decades of land use changes on soil quality and biomass productivity in a Mediterranean landscape in Chile. *Catena* 140, 195–204. <https://doi.org/10.1016/j.catena.2016.01.029>.
- Hissler, C., Probst, J.L., 2006. Chlor-alkali industrial contamination and riverine transport of mercury: distribution and partitioning of mercury between water, suspended matter, and bottom sediment of the Thur River, France. *Appl. Geochem.* 21, 1837–1854. <https://doi.org/10.1016/j.apgeochem.2006.08.002>.
- Hissler, C., Hostache, R., Iffly, J.F., Pfister, L., Stille, P., 2015. Anthropogenic rare earth element fluxes into floodplains: coupling between geochemical monitoring and hydrodynamic-sediment transport modelling. *Compt. Rendus Geosci.* 347, 294–303. <https://doi.org/10.1016/j.crte.2015.01.003>.
- Hissler, C., Stille, P., Iffly, J.F., Guignard, C., Chabaux, F., Pfister, L., 2016. Origin and dynamics of Rare Earth Elements during flood events in contaminated river basins: Sr-Nd-Pb evidence. *Environ. Sci. Technol.* 50, 4624–4631. <https://doi.org/10.1021/acs.est.5b03660>.
- IBGE, 2010. Dados do Censo. Diário Oficial da União, Brasília, DF, 04 nov. 2010. http://www.ibge.gov.br/censo2010/dados_divulgados/index.php?uf=35 (accessed 10 December 2013).
- IPT, 2006. Relatório Zero da Bacia do Sorocaba e Médio Tietê – Atualização 2005. Relatório Técnico n° 80 401–205. IPT, São Paulo.
- Johnson, N.M., Likens, G.E., Bormann, F.H., Pierce, P.S., 1968. Rate of chemical weathering of silicate minerals in New Hampshire. *Geochim. Cosmochim. Acta* 32, 531–545. [https://doi.org/10.1016/0016-7037\(68\)90044-6](https://doi.org/10.1016/0016-7037(68)90044-6).
- Karamesouti, M., Detsis, V., Kounalaki, K., Vassiliou, P., Salvati, L., Kosmas, C., 2015. Land-use and land degradation processes affecting soil resources: evidence from a traditional Mediterranean cropland (Greece). *Catena* 132, 45–55. <https://doi.org/10.1016/j.catena.2015.04.010>.
- Keene, W.C., Pszenny, A.A.P., Galloway, J.N., Hawley, M.E., 1986. Sea-Salt corrections and interpretation of constituent ratios in marine precipitation. *J. Geophys. Res.* 91 (D6), 6647–6658. <https://doi.org/10.1029/JD091iD06p6647>.
- Kim, S.M., Jang, T.I., Kang, M.S., Im, S.J., Park, S.W., 2014. GIS-based lake sediment budget estimation taking into consideration land use change in an urbanizing catchment area. *Environ. Earth Sci.* 71, 2155–2165. <https://doi.org/10.1007/s12665-013-2621-7>.
- Köppen, W., 1948. *Climatologia*. Fondo de Cultura Económica, México.

- Kosmas, C., Karamesouti, M., Kounalaki, K., Detsis, V., Vassiliou, P., Salvati, L., 2016. Land degradation and long-term changes in agro-pastoral systems: Na empirical analysis of ecological resilience in Asteroussia – Crete (Greece). *Catena* 147, 169–2004. <https://doi.org/10.1016/j.catena.2016.07.018>.
- Lasaga, A.C., Soler, J.M., Ganor, J., Burch, T.E., Nagy, K.L., 1994. Chemical weathering rate laws and global geochemical cycles. *Geochim. Cosmochim. Acta* 58 (10), 2361–2386. [https://doi.org/10.1016/0016-7037\(94\)90016-7](https://doi.org/10.1016/0016-7037(94)90016-7).
- Latocha, A., 2009. Land-use changes and longer-term human–environment interactions in a mountain region (Sudetes Mountains, Poland). *Geomorphology* 108, 48–57. <https://doi.org/10.1016/j.geomorph.2008.02.019>.
- Latocha, A., Migon, P., 2006. Geomorphology of medium-high mountains under changing human impact: from managed slopes to nature restoration; a study from the Sudetes, SW Poland. *Earth Surf. Process. Landforms* 31, 1657–1673. <https://doi.org/10.1002/esp.1437>.
- Latocha, A., Szymonowski, M., Jeziorska, J., Stec, M., Roszczewska, M., 2016. Effects of land abandonment and climate change on soil erosion – an example from depopulated agricultural lands in the Sudetes Mts., SW Poland. *Catena* 145, 128–141. <https://doi.org/10.1016/j.catena.2016.05.027>.
- Latrubesse, E.M., Amisler, M.L., de Moraes, R.P., Aquino, S., 2009. The geomorphologic response of a large pristine alluvial river to tremendous deforestation in the South American tropics: the case of the Araguaia River. *Geomorphology* 113, 239–252. <https://doi.org/10.1016/j.geomorph.2009.03.014>.
- Louvat, P., Allègre, C.J., 1997. Present denudation rates on the island of Réunion determined by river geochemistry: basalt weathering and mass budget between chemical and mechanical erosions. *Geochim. Cosmochim. Acta* 61, 3645–3669. [https://doi.org/10.1016/S0016-7037\(97\)00180-4](https://doi.org/10.1016/S0016-7037(97)00180-4).
- Louvat, P., Allègre, C.J., 1998. Riverine erosion rates on Sao Miguel volcanic island, Azores archipelago. *Chem. Geol.* 148, 177–200. [https://doi.org/10.1016/S0009-2541\(98\)00028-X](https://doi.org/10.1016/S0009-2541(98)00028-X).
- Louvat, P., Gislasen, S.R., Allègre, C.J., 2008. Chemical and mechanical erosion rates in Iceland as deduced from river dissolved and solid material. *Am. J. Sci.* 308, 679–726. <https://doi.org/10.2475/05.2008.02>.
- Lupinacci, C.M., Conceição, F.T., Simon, A.L.H., Perez Filho, A., 2017. Land use changes due to energy policy as a determining factor for morphological processes in fluvial systems in São Paulo State, Brazil. *Earth Surf. Process. Landforms* 42, 2402–2413. <https://doi.org/10.1002/esp.4200>.
- Martin, J.M., Meybeck, M., 1979. Elemental mass-balance of material carried by major world rivers. *Mar. Chem.* 7 (3), 173–206. [https://doi.org/10.1016/0304-4203\(79\)90039-2](https://doi.org/10.1016/0304-4203(79)90039-2).
- Meybeck, M., 1987. Global chemical weathering of surficial rocks estimated from river dissolved loads. *Am. J. Sci.* 287, 401–428. <https://doi.org/10.2475/ajs.287.5.401>.
- Meybeck, M., Laroche, L., Dürr, H.H., Syvitski, J.P.M., 2003. Global variability of daily total suspended solids and their fluxes in rivers. *Glob. Planet. Change* 39, 65–93. [https://doi.org/10.1016/S0921-8181\(03\)00018-3](https://doi.org/10.1016/S0921-8181(03)00018-3).
- Mhangara, P., Kakembo, V., Lim, K.J., 2012. Soil erosion risk assessment of the Keiskamma catchment, South Africa using GIS and remote sensing. *Environ. Earth Sci.* 65, 2087–2102. <https://doi.org/10.1007/s12665-011-1110-x>.
- Millot, R., Gaillardet, J., Duprè, B., Allègre, C.J., 2002. The global control of silicate weathering rates and the coupling with physical erosion: new insights from rivers of Canadian Shield. *Earth Planet. Sci. Lett.* 196, 83–98. [https://doi.org/10.1016/S0012-821X\(01\)00599-4](https://doi.org/10.1016/S0012-821X(01)00599-4).
- Minella, J.P.G., Merten, G.H., Walling, D.E., Reichert, J.M., 2009. Changing sediment yield as an indicator of improved soil management practices in southern Brazil. *Catena* 79, 228–236. <https://doi.org/10.1016/j.catena.2009.02.020>.
- BRASIL. Ministério das Minas e Energia, 1983. *Projeto RADAMBRASIL Folhas 23/24, Rio de Janeiro*. Levantamento de Recursos Naturais 32, 27–247.
- Montgomery, D.R., 2007. Soil erosion and agricultural sustainability. *PNAS* 104, 13268–13272. <https://doi.org/10.1073/pnas.0611508104>.
- Moon, S., Chamberlain, C.P., Hilley, G.E., 2014. New estimates of silicate weathering rates and their uncertainties in global rivers. *Geochim. Cosmochim. Acta* 134, 257–274. <https://doi.org/10.1016/j.gca.2014.02.033>.
- Moraes, I.C., Conceição, F.T., Cunha, C.M.L., Moruzzi, R.B., 2012. Interferência do uso da Terra nas inundações da área urbana do córrego da servidão, Rio Claro (SP). *Rev. Bras. Geomorfologia* 13 (2), 187–200.
- Moreira-Nordemann, L.M., Girardi, P., Ré Poppi, N., 1997. Química da precipitação atmosférica na cidade de Campo Grande – MS. *Rev. Bras. Geofis.* 15 (1), 35–44. <https://doi.org/10.1590/S0102-261X1997000100004>.
- Mortatti, J., Probst, J.L., 2003. Silicate rock weathering and atmospheric/soil CO₂ uptake in the Amazon basin estimated from river water geochemistry: seasonal and spatial variations. *Chem. Geol.* 197, 177–196. [https://doi.org/10.1016/S0009-2541\(02\)00349-2](https://doi.org/10.1016/S0009-2541(02)00349-2).
- Mortatti, J., Probst, J.L., Ferreira, J.R., 1992. Hydrological and geochemical characteristics of the Jamari and Jiparana river basin (Rondonia, Brazil). *Geol.* 26 (3), 287–296. <https://doi.org/10.1007/BF02629808>.
- Mortatti, J., Victoria, R.L., Tardy, Y., 1997. Balanço de alteração e erosão química na bacia amazônica. *Geochim. Bras.* 11 (1), 2–13.
- Mortatti, J., Vendramini, D., Oliveira, H., 2012. Avaliação da poluição doméstica fluvial na zona urbana do município de Piracicaba, SP, Brasil. *Rev. Ambient. Água* 7 (2), 110–119. <https://doi.org/10.4136/ambi-água.846>.
- Mosello, R., Bianchi, M., Geiss, H., Marchetto, A., Serrini, G., Serini Lanza, G., Tartari, G.A., Muntau, H., 1996. *AQUACON-MedBas Subproject No. 6: Acid Rain Analysis*. Environment Institute, Luxembourg.
- Mugagga, F., Kakembo, V., Buyinza, M., 2012. Land use changes on the slopes of Mount Elgon and the implications for the occurrence of landslides. *Catena* 90, 39–46. <https://doi.org/10.1016/j.catena.2011.11.004>.
- Murray, A.B., Lazarus, E., Ashton, A., Baas, A., Coco, G., Coulthard, T., Fonstad, M., Haff, P., McNamara, D., Paola, C., Pelletier, J., Reinhardt, L., 2009. *Geomorphology* 103, 496–505. <https://doi.org/10.1016/j.geomorph.2008.08.013>.
- Négrel, P., Roy, S., Petelet-Giraud, E., Millot, R., Brenot, A., 2007. Long-term fluxes of dissolved and suspended matter in the Ebro River Basin (Spain). *J. Hydrol.* 342, 249–260. <https://doi.org/10.1016/j.jhydrol.2007.05.013>.
- Oliva, P., Viers, J., Duprè, B., 2003. Chemical weathering in granitic environments. *Chem. Geol.* 202, 225–256. <https://doi.org/10.1016/j.chemgeo.2002.08.001>.
- Oliveira, J.B., Camargo, M.N., Rossi, M., Calderano Filho, B. (1999) Mapa pedológico do Estado de São Paulo: legenda expandida. Campinas: Instituto Agronômico; Rio de Janeiro: Embrapa-Solos. 64p.: mapa.
- Oliveira, P.T.S., Nearing, M.A., Wendland, E., 2015. Orders of magnitude increase in soil erosion associated with land use changes from native to cultivated vegetation in a Brazilian savannah environment. *Earth Surf. Process. Landforms* 40, 1524–1532. <https://doi.org/10.1002/esp.3738>.
- Pedro, G., 1966. *Essaísur lacaracterisaçãogêochimiquedesdiferentesprocessoszonauxrésultant de l'altération de rochessuperficiales (cyclealuminossilicique)*. C. R. Acad. Sci. Paris 262, 1821–1831.
- Peray, N., 1998. *Composition chimique des eaux e l'III à Strasbourg: variations saisonnières des flux de matières et bilan de l'erosion chimique*. ULP, Centre de Géochimie de la Surface (Report), Strasbourg.
- Perez Filho, A., Quaresma, C.C., 2011. Ação antrópica sobre as escalas temporais dos fenômenos geomorfológicos. *Rev. Bras. Geomorfologia* 12, 83–90. <https://doi.org/10.20502/rbg.v12i0.261>.
- Perrotta, M.M., Salvador, E.D., Lopes, R.C., D'Agostinho, L.Z., Peruffo, N., Gomes, S.D., Sachs, L.L.B., Meira, V.T., Garcia, M.G.M., Lacerda Filho, J.V., 2005. Mapa geológico do Estado de São Paulo, escala 1:750.000. Programa Geologia do Brasil – PGB, CPRM, São Paulo.
- Probst, J.L., 1986. Dissolved and suspended matter transported by the Girou River (France): mechanical e chemical erosion rates in a calcareous molasse basin. *Hydrol. Sci. J.* 31, 61–79. <https://doi.org/10.1080/02626668609491028>.
- Probst, J.L., 1992. *Géochimie et Hydrologie de l'Erosion Continentale. Mécanismes Bilan Global Actuel et Fluctuations au Cours des 500 Derniers millions d'années*. Sci. Géol. Mém. 94, Strasbourg.
- Probst, J.L., Nkounkou, R.R., Krempp, G., Bricquet, J.P., Thiébaux, J.P., Olivry, J.C., 1992. Dissolved major elements exported by the Congo and the Ubangui rivers during the period 1987–1989. *J. Hydrol.* 135, 237–257. [https://doi.org/10.1016/0022-1694\(92\)90090-1](https://doi.org/10.1016/0022-1694(92)90090-1).
- Probst, J.L., Mortatti, J., Tardy, Y., 1994. Carbon river fluxes and global weathering CO₂ consumption in the Congo and Amazon river basins. *Appl. Geochem.* 9, 1–13. [https://doi.org/10.1016/0883-2927\(94\)90047-7](https://doi.org/10.1016/0883-2927(94)90047-7).
- Ribani, M., Bottoli, C.B.G., Collins, C.H., Jardim, I.C.S.F., Melo, L.F.C., 2004. *Validação em métodos cromatográficos e eletroforéticos*. *Quím. Nova* 27 (5), 771–780.
- Riffel, S.B., Vasconcelos, P.M., Carmo, I.O., Farley, K.A., 2015. Combined ⁴⁰Ar/³⁹Ar and (U-Th)/He geochronological constraints on long-term landscape evolution of the Second Paraná Plateau and its ruiniform surface features, Paraná, Brazil. *Geomorphology* 233, 52–63. <https://doi.org/10.1016/j.geomorph.2014.10.041>.
- Rodrigues, C., 2005. *Morfologia original e morfologia antropogênica na definição de unidades espaciais de Planejamento Urbano: exemplo da metrópole paulista*. *Rev. Dep. Geograf.* 17, 101–111. <https://doi.org/10.7154/RDG.2005.0017.0008>.
- Rosolen, V., Campos, A.B., Govone, S.J., Rocha, C., 2015. Contamination of wetland soils and floodplain sediments from agricultural activities in the Cerrado Biome (State of Minas Gerais, Brazil). *Catena* 128, 203–210. <https://doi.org/10.1016/j.catena.2015.02.007>.
- Ross, J.L.S., 1985. *Relevo Brasileiro: Uma nova proposta de Classificação*. *Revista do Departamento de Geografia* 4, 25–39. <https://doi.org/10.7154/RDG.1985.0004.0004>.
- Ross, J.L.S., Moroz, I.C., 1997. *Mapa geomorfológico do Estado de São Paulo*. Laboratório de Geomorfologia, Depto Geografia, FFLCH-USP, Laboratório de Cartografia Geotécnica – Geologia Aplicada – IPT, FAPESP. Mapas e Relatórios – SP, São Paulo.
- Sanyal, J., Densmore, A.L., Caronneau, P., 2014. Analysing the effect of land-use/cover changes at sub-catchment levels on downstream flood peaks: a semi-distributed modelling approach with sparse data. *Catena* 118, 28–40. <https://doi.org/10.1016/j.catena.2014.01.015>.
- Sardinha, D.S., Conceição, F.T., Bonotto, D.M., Salles, M.H.F., Angelucci, V.A., 2008. *Avaliação do balanço anual de cátions e ânions na bacia do Alto Sorocaba (SP)*. *Rev. Bras. Geosci.* 38 (2), 730–740.
- Serpa, D., Nunes, J.P., Santos, J., Sampaio, E., Jacinto, R., Veiga, S., Abrantes, N., 2015. Impacts of climate and land use changes on the hydrological and erosion processes of two contrasting Mediterranean catchments. *Sci. Total Environ.* 538, 64–77. <https://doi.org/10.1016/j.scitotenv.2015.08.033>.
- Simon, A.L.H., Cunha, C.M.L., 2008. Alterações geomorfológicas derivadas da intervenção de atividades antrópicas: análise temporal na bacia do Arroio Santa Bárbara – Pelotas (RS). *Rev. Bras. Geomorfologia* 9 (2), 29–38. <https://doi.org/10.20502/rbg.v9i2.107>.
- Spatti Júnior, E.P., Conceição, F.T., Fernandes, A.M., Sardinha, D.S., Moruzzi, R.B., 2019. Chemical weathering rates of clastic sedimentary rocks from the Paraná Basin in the Paulista Peripheral Depression, Brazil. *J. South Am. Earth Sci.* 96, 102369. <https://doi.org/10.1016/j.jsames.2019.102369>.
- Stallard, R.F., Edmond, J.M., 1981. Geochemistry of the Amazon Basin. 1. Precipitation chemistry and marine contribution to the dissolved load at the time of peak discharge. *J. Geophys. Res. Serie C* 86(10), 9844–9858. 203–210. <https://doi.org/10.1029/JC086iC10p09844>.
- Stallard, R.F., Edmond, J.M., 1987. Geochemistry of the Amazon Basin. 3. Weathering chemistry and limits to dissolved inputs. *J. Geophys. Res. Serie C* 92 (8), 8293–8302. <https://doi.org/10.1029/JC092iC08p08293>.
- Summerfield, M.A., 1991. *Global Geomorphology*. Longman and Wiley, Harlow, England and New York.
- Sun, W., Shao, Q., Liu, J., Zhai, J., 2014. Assessing the effects of land use and topography on soil erosion on the Loess Plateau in China. *Catena* 121, 151–163. <https://doi.org/10.1016/j.catena.2014.05.009>.
- Tardy, Y., 1968. *Une méthode de détermination des types d'altération actuels par l'étude des eaux en pays granitiques et gneissiques*. C. R. Acad. Sci. Serie D 267, 579–582.

- Tardy, Y., 1969. *Geochimie des alterations. Etudes des arènes et des eaux de quelques massifs cristallins d'Europe et d'Afrique*. Mém. Serv. Carte Géol. Als Lorraine 31.
- Tardy, Y., 1971. Characterization of the principal weathering types by the geochemistry of waters from some European and African crystalline massifs. *Chem. Geol.* 7, 253–271. [https://doi.org/10.1016/0009-2541\(71\)90011-8](https://doi.org/10.1016/0009-2541(71)90011-8).
- Tarolli, P., Sofia, G., 2016. Human topographic signatures and derived geomorphic processes across landscapes. *Geomorphology* 225, 140–161. <https://doi.org/10.1016/j.geomorph.2015.12.007>.
- Tchobanoglous, G., Burton, F.L., 1991. *Wastewater Engineering: Treatment, Disposal and Reuse/Metcalf and Eddy*. 3rd ed. McGraw-Hill, New York (1334 p).
- USDA, United States Department of Agriculture, 1999. *Soil Taxonomy – A Basic System of Soil Classification for Making and Interpreting Soils Surveys*. 2nd ed. US Department of Agricultural Soil Conservation Service, Washington DC (754 p).
- USGS, October 2011. Shuttle Radar Topographic Mission.
- Van Rompaey, A.J.J., Govers, G., Puttemans, C., 2002. Modelling land use changes and their impact on soil erosion and sediment supply to rivers. *Earth Surf. Process. Landforms* 27, 481–494. <https://doi.org/10.1002/esp.335>.
- Walling, D.E., Fang, D., 2003. Recent trends in the suspended sediment loads of the world's rivers. *Glob. Planet. Change* 39, 111–126. [https://doi.org/10.1016/S0921-8181\(03\)00020-1](https://doi.org/10.1016/S0921-8181(03)00020-1).
- West, A.J., Galy, A., Bickle, M., 2005. Tectonic and climatic controls on silicate weathering. *Earth Planet. Sci. Lett.* 235, 211–228. <https://doi.org/10.1016/j.epsl.2005.03.020>.
- White, A.F., Blum, A.E., 1995. Effects of climate on chemical weathering in watersheds. *Geochim. Cosmochim. Acta* 59, 1729–1747. [https://doi.org/10.1016/0016-7037\(95\)00078-E](https://doi.org/10.1016/0016-7037(95)00078-E).
- Wilson, T.R.S., 1975. Salinity and the major elements of sea water. In: Riley, J.P., Skirrow, G. (Eds.), *Chemical Oceanography*, 2nd Ed Academic, Florida, pp. 365–413.
- Zhang, Y., Shanggaun, Z., 2016. The change of soil water storage in three land use types after 10 years on the Loess Plateau. *Catena* 147, 87–95. <https://doi.org/10.1016/j.catena.2016.06.036>.
- Zope, P.E., Eldho, T.I., Jothiprakash, V., 2016. Impacts of land use-land cover change and urbanization on flooding: a case study of Oshiwara River basin in Mumbai, India. *Catena*. 145, 142–154. <https://doi.org/10.1016/j.catena.2016.06.009>.